On the Accuracy of Equivalent Circuit Models for Multi-Antenna Systems

Jon W. Wallace, *Member, IEEE*, and Rashid Mehmood, *Student Member, IEEE*

***Abstract*—The equivalent circuit model of a general PEC antenna array is derived, based on a rigorous method of moments (MOM) formulation, indicating that network analysis is exact from the standpoint of electromagnetic wave theory. It is found that the network parameters (Z, Y, or S-parameters) for the transmit mode can be used for exact prediction of the receive-mode array response. Numerical and experimental examples illustrate the validity of the analytical results.**

***Index Terms*—Antenna arrays, equivalent circuits, modeling, moment methods, multiple-input multiple-output (MIMO) systems, mutual coupling.**

I. Introduction

EQUIVALENT circuit models, also referred to as network models, have gained attention for modeling antenna arrays and multiple-input multiple-output (MIMO) systems, allowing circuit effects such as amplifier noise, matching and reconfigurability to be studied [1]–[5]. Such models are computationally attractive, since the transmit and receive arrays can be represented as equivalent circuits, requiring only a modest number of full-wave simulations or measurements, after which circuits of varying complexity are analyzed with efficient circuit-level simulation. In [6] it was formally proven that antenna arrays in the transmit and receive mode can be modeled with network analysis and that the same impedance matrix (with the exception of a transpose) can be used for both modes. In [7], the effect of mutual coupling on adaptive arrays is studied by considering an equivalent network model, yielding a simple linear relationship between the loaded and open-circuit voltages on a receive array and a beamformer for optimal signal to interference and noise ratio (SINR) is derived. More recently, [8] gives the equivalent circuit of a single receive antenna and [9] provides an equivalent circuit for a receiving array.

In contrast to work endorsing simple equivalent circuit models, there is also work that questions the use of such models. For example, [10] suggests that the compensation method in [7] is suboptimal since the network model only assumes a single basis function per antenna and an improved compensation method based on a full moment method model of the array is proposed. In [11] the use of Norton or Thévenin equivalent circuits for receiving antennas is challenged, since power absorbed by the internal impedance of the network does not have a strict physical meaning and a different model is proposed based on a constant power source. A physically appealing model is also proposed in [12] that includes the transmit antenna in the equivalent receive model. Recent work [13], [14] also questions the use of array transmit-mode mutual impedances for the receive mode, which is troubling from the standpoint of reciprocity.

The purpose of this paper is to provide a straightforward but rigorous analysis of antenna arrays based on method of moments (MOM), illustrating that equivalent circuit models are exact and that receive-mode behavior of an array can be exactly predicted by usual transmit-mode quantities. Although these observations are basically equivalent to those in [6], the MOM analysis here has a number of advantages: the development is simpler and intuitive, the transmit and receive modes do not need to be considered separately and the MOM discretization provides an exact definition for the ports. The analysis provides valuable insight on the operation of equivalent circuit models, such as the connection of transmit and receive mode, the number of basis functions (or degrees of freedom) required to represent currents accurately on an antenna array and potential sources of inaccuracy in network models. Several examples are provided based on full-wave simulations and direct measurement that validate the analytical results.

The paper is organized as follows: Section II derives Z, Y and S-parameter equivalent circuit models of antenna arrays in the transmit/receive mode from MOM. Section III provides numerical examples that demonstrate the observations of the MOM analysis, followed by an experimental example in Section IV. Section V provides concluding remarks.

II. Method of Moments Analysis of Multi-Element Arrays

In this section, we rigorously analyze general antenna arrays accessible at a finite set of N_P ports by applying the method of moments. Although we restrict our attention to antennas composed of perfect electric conductor (PEC) surfaces, we do so only for the sake of simplicity and the method can be naturally extended to dielectric and magnetic materials, finite conductivity, etc. This exercise provides valuable intuition on the connection between network analysis and full-wave analysis and the requirements for good agreement. Furthermore, we prove that mutual interactions of the transmit mode, receive mode and combined transmit/receive mode can be captured with a single equivalent model that involves the usual (transmit mode) mutual impedance matrix.

Manuscript received June 15, 2010; revised November 03, 2010; accepted November 15, 2010. Date of publication May 10, 2011; date of current version February 03, 2012.

The authors are with the School of Engineering and Science, Jacobs University Bremen, Bremen, Germany (e-mail: wall@ieee.org; r.mehmood@ieee.org).

Color versions of one or more of the figures in this paper are available online at http://ieeexplore.ieee.org.

Digital Object Identifier 10.1109/TAP.2011.2152339

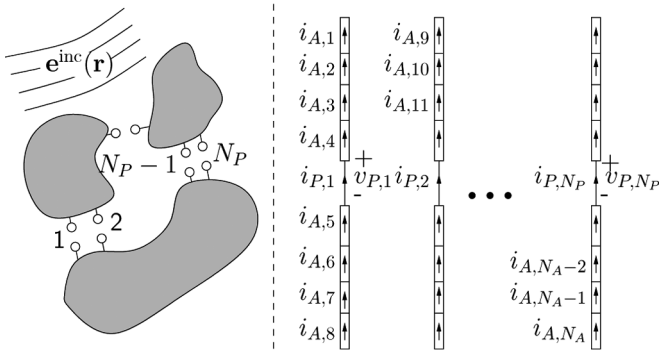

Fig. 1. Geometry of (a) a general antenna array and (b) a wire dipole array and example method of moments segmentation.

A. Governing Equations

Fig. 1 depicts a general antenna array in a free-space medium where signals can be driven and/or measured at N_P ports. An externally applied incident field may also be present, denoted by $\mathbf{e}^{\text{inc}}$, which is general (plane wave, spherical wave, etc.).

Total field at observation point $\mathbf{r}$ is given in terms of current density $\mathbf{j}(\mathbf{r})$ on the antenna according to [15]

$$\mathbf{e}(\mathbf{r}) = \mathbf{e}^{\text{inc}}(\mathbf{r}) + \int \mathbf{G}(\mathbf{r},\mathbf{r}')\mathbf{j}(\mathbf{r}')d\mathbf{r}' \tag{1}$$

where $\mathbf{G}(\mathbf{r},\mathbf{r}')$ is the dyadic Green's function for free space. MOM discretization is performed using basis expansion $\mathbf{j}(\mathbf{r}) = \sum_n i_n \mathbf{f}_n(\mathbf{r})$, or

$$\mathbf{e}(\mathbf{r}) = \mathbf{e}^{\text{inc}}(\mathbf{r}) + \sum_{n=1}^{N_B} i_n \underbrace{\int \mathbf{G}(\mathbf{r},\mathbf{r}')\mathbf{f}_n(\mathbf{r}')d\mathbf{r}'}_{\{\cdot\}_k = M_{kn}(\mathbf{r})} \tag{2}$$

followed by the projection onto the weighting functions $\mathbf{w}_n(\mathbf{r})$

$$\underbrace{\int \mathbf{w}_m^T(\mathbf{r})\mathbf{e}(\mathbf{r})d\mathbf{r}}_{v_m} = \underbrace{\int \mathbf{w}_m^T(\mathbf{r})\mathbf{e}^{\text{inc}}(\mathbf{r})d\mathbf{r}}_{v_m^{\text{inc}}} + \sum_{n=1}^{N_B} i_n \underbrace{\int\int \mathbf{w}_m^T(\mathbf{r})\mathbf{G}(\mathbf{r},\mathbf{r}')\mathbf{f}_n(\mathbf{r}')d\mathbf{r}'d\mathbf{r}}_{q_{mn}} \tag{3}$$

which gives the usual linear relationship

$$\mathbf{v} = \mathbf{v}^{\text{inc}} + \mathbf{Q}\mathbf{i}. \tag{4}$$

We choose $\mathbf{f}_n(\mathbf{r})$ and $\mathbf{w}_n(\mathbf{r})$ to have identical local support $\mathbf{r} \in \Omega_n$, such that i_n and v_n represent the current and voltage on the nth element, respectively.

The basis functions are ordered so that the first N_P correspond to port terminals, where i_n and v_n for $n \in \{1,\ldots,N_P\}$ are the port currents and voltages. Many choices of the $\mathbf{f}_n(\mathbf{r})$ and $\mathbf{w}_n(\mathbf{r})$ are possible, but a simple choice is a filament properly connecting the two port terminals, where i_n is the current on the filament and v_n is the contour integral for voltage between the terminals. Note that basis and weighting functions for elements on the PEC structure are chosen to be tangential to these surfaces.

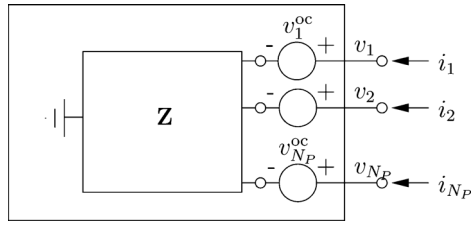

Fig. 2. Equivalent antenna array circuit model in transmit/receive mode.

Appropriately partitioning (4) into elements at the ports (P) and on the PEC antenna array structure (A),

$$\mathbf{v}_P = \mathbf{v}_P^{\text{inc}} + \mathbf{Q}_{PP}\mathbf{i}_P + \mathbf{Q}_{PA}\mathbf{i}_A \tag{5}$$

$$\mathbf{v}_A = \mathbf{v}_A^{\text{inc}} + \mathbf{Q}_{AP}\mathbf{i}_P + \mathbf{Q}_{AA}\mathbf{i}_A = 0 \tag{6}$$

where $\mathbf{v}_A = 0$ due to PEC surfaces.

B. General Transmit/Receive Mode

The general mode (transmit and receive) of the antenna is considered. From (6) the currents on the antenna array are

$$\mathbf{i}_A = -\mathbf{Q}_{AA}^{-1}\mathbf{v}_A^{\text{inc}} - \mathbf{Q}_{AA}^{-1}\mathbf{Q}_{AP}\mathbf{i}_P \tag{7}$$

and plugging into (5) gives the voltages on the ports in terms of the port currents only, or

$$\mathbf{v}_P = \underbrace{\mathbf{v}_P^{\text{inc}} - \mathbf{Q}_{PA}\mathbf{Q}_{AA}^{-1}\mathbf{v}_A^{\text{inc}}}_{\mathbf{v}_P^{\text{oc}}} + \underbrace{(\mathbf{Q}_{PP} - \mathbf{Q}_{PA}\mathbf{Q}_{AA}^{-1}\mathbf{Q}_{AP})}_{\mathbf{Z}}\mathbf{i}_P. \tag{8}$$

This resulting system is equivalent to the network model depicted in Fig. 2. Thus, the operation of the array can be computed exactly if we know the open circuit voltages $\mathbf{v}^{\text{oc}}$ for all incident fields of interest as well as the impedance matrix $\mathbf{Z}$.

Radiated fields from the antenna can be computed using (2), where the partitioning $\mathbf{M}(\mathbf{r}) = [\mathbf{M}_P(\mathbf{r})\ \mathbf{M}_A(\mathbf{r})]$ yields

$$\begin{aligned}\mathbf{e}(\mathbf{r}) &= \mathbf{e}^{\text{inc}}(\mathbf{r}) + \mathbf{M}_A\mathbf{i}_A + \mathbf{M}_P\mathbf{i}_P \\ &= \mathbf{e}^{\text{inc}}(\mathbf{r}) - \underbrace{\mathbf{M}_A\mathbf{Q}_{AA}^{-1}\mathbf{v}_A^{\text{inc}}}_{-\mathbf{e}^{\text{oc,scat}}(\mathbf{r})} \\ &\quad + \underbrace{(\mathbf{M}_P - \mathbf{M}_A\mathbf{Q}_{AA}^{-1}\mathbf{Q}_{AP})}_{\mathbf{E}^{\text{oc}}(\mathbf{r})}\mathbf{i}_P\end{aligned} \tag{9}$$

where $\mathbf{e}^{\text{oc,scat}}$ is field scattered by the antenna for $\mathbf{i}_P = 0$ (open circuit) and $e_{kn}^{\text{oc}}(\mathbf{r})$ is interpreted as the radiation pattern of port n for polarization k for unit input current when the other ports are open-circuited. Typically, we are most interested in far-fields of the array and the expression can be simplified to

$$\mathbf{e}(\mathbf{r}) = \mathbf{e}^{\text{inc}}(\mathbf{r}) + [\mathbf{E}^{\text{oc}}(\hat{r})\mathbf{i}_P + \mathbf{e}^{\text{oc,scat}}(\hat{r})]\exp\frac{(-jkr)}{r}. \tag{10}$$

In the transmit mode, $\mathbf{e}^{\text{inc}} = 0$, $\mathbf{v}_S^{\text{inc}} = 0$ and $\mathbf{e}^{\text{oc,scat}} = 0$ so that the radiated fields are just a superposition of the open-circuit embedded patterns weighted by the port currents. For the receive mode (and combined mode) the scattered field term must also be included.

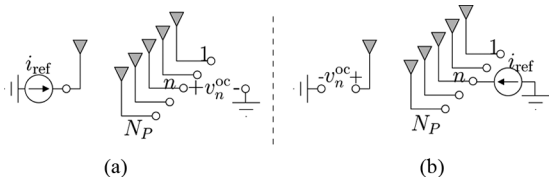

Fig. 3. Computation of $v_n^{\rm oc}$ for far-field sources (a) direct problem and (b) reciprocal equivalent.

C. Comparison of Transmit and Receive Mode

Our analysis shows that the only difference in using the antenna in transmit versus receive mode is that for the pure transmit case, $\mathbf{v}^{\rm oc} = 0$ so that a linear system is obtained, whereas $\mathbf{v}^{\rm oc} \neq 0$ for the receive case. Also, note that $\mathbf{Z}$ is the usual transmit mutual impedance and there is no approximation when using this for the receive case. This is in contrast to the development in [13] that questions the use of transmit mutual impedances for the receive mode.

We also compare with the result in [6], where it was shown that the receive mode mutual impedance matrix is the transpose of that for the transmit mode. Although a reciprocal antenna and medium are considered here, the same equivalent circuit as in Fig. 2 would be obtained for non-reciprocal (general bianisotropic) materials. The impedance matrix does not transpose due to $\mathbf{e}^{\rm inc}$ or what is connected to the ports, indicating that $\mathbf{Z}$ must be the same for both the transmit and receive mode.

To remedy the apparent dilemma, it must be noted that [6] invokes the Lorentz reciprocity theorem, where for non-reciprocal materials the system must be changed to a new system with complementary materials [15]. Given that the original transmit impedance matrix is $\mathbf{Z}$, we denote the transmit impedance matrix of the complementary system as $\mathbf{Z}^C$. In [6] it was actually shown that whereas $\mathbf{Z}$ is used for the transmit case, $(\mathbf{Z}^C)^T$ should be used for the receive case. However, since the original and complementary systems are related by reciprocity, $\mathbf{Z} = (\mathbf{Z}^C)^T$ and $\mathbf{Z}$ alone (no transpose) can be used for the receive system. Also, [6] shows that the load matrix $\mathbf{Z}_L = (\mathbf{Z}^C)^*$ is optimal for receive power transfer, but this is the same as a Hermitian match to the original physical transmit impedance, or $\mathbf{Z}_L = \mathbf{Z}^H$. For S-parameters with a real normalizing impedance, it can be shown that this condition is the same as $\mathbf{S}_L = \mathbf{S}^H$, which was proven to provide maximum power transfer in [2].

D. Computation of $v^{\rm oc}$

The exact network model requires knowledge of $\mathbf{v}^{\rm oc}$ for all incident fields $\mathbf{e}^{\rm inc}(\mathbf{r})$ of interest. In many cases, external sources are far away from the array and $\mathbf{v}^{\rm oc}(\hat{r})$ only needs to be found for plane-wave incidence. In this case, reciprocity arguments can be used to obtain $\mathbf{v}^{\rm oc}(\hat{r})$ in terms of the radiated far-fields for the transmit-only mode.

Consider the configuration depicted in Fig. 3(a) for finding $\mathbf{v}^{\rm oc}(\hat{r})$, which is the open-circuit voltage induced on the array due to a plane wave originating from direction $\hat{r}$. Here, a transmit reference antenna is placed at coordinate $\mathbf{r}$, which is in the far-field of the array near the origin and driven with current $i_{\rm ref}$. If we use a simple Hertzian dipole for the reference antenna, the field present at the origin is

$$\mathbf{e}_0 = \hat{\ell} j\ell i_{\rm ref} k\eta \frac{\exp(-jkr)}{4\pi r} \tag{11}$$

where $\hat{\ell}$ is the orientation and ℓ the effective length of the reference antenna and k and η are the wavenumber and intrinsic impedance of the background medium.

Next, consider the reciprocal system in Fig. 3(b), which will give the same value of $v_n^{\rm oc}$. The field incident on the reference antenna is

$$\mathbf{e}^{\rm inc}(\mathbf{r}) = \mathbf{e}_n^{\rm oc}(\hat{r}) i_{\rm ref} \exp\frac{(-jkr)}{r}. \tag{12}$$

The open-circuit voltage on the Hertzian dipole is

$$\begin{aligned} v_0^{\rm oc}(\hat{r}) &= -\mathbf{e}^{\rm inc}(\mathbf{r}) \cdot \hat{\ell}\ell = -\mathbf{e}_n^{\rm oc}(\hat{r}) \cdot \underbrace{\hat{\ell}\ell i_{\rm ref} \exp\frac{(-jkr)}{r}}_{-j4\pi \mathbf{e}_0/(k\eta)} \\ &= \underbrace{\frac{j4\pi}{k\eta}}_{\alpha} \mathbf{e}_0^T \mathbf{e}^{\rm oc}(\hat{r}) = v_n^{\rm oc}(\hat{r}). \end{aligned} \tag{13}$$

Thus, the receive-mode open-circuit voltages for plane-wave incidence can be computed using the transmit-mode open-circuit embedded radiation patterns.

For receive array calibration, the direct arrangement in Fig. 3(a) may be preferred. Terminating the array with load impedance matrix $\mathbf{Z}_L$ and defining $\mathbf{i}$ to be the vector of currents flowing into the antenna ports,

$$\mathbf{v} = \mathbf{v}^{\rm oc} + \mathbf{Z}\mathbf{i} \tag{14}$$

$$\mathbf{v} = -\mathbf{Z}_L \mathbf{i}. \tag{15}$$

Proper combination gives

$$\mathbf{v}^{\rm oc} = (\mathbf{I} + \mathbf{Z}\mathbf{Z}_L^{-1})\mathbf{v} \tag{16}$$

indicating that the open-circuit voltage can be computed using a measurable voltage $\mathbf{v}$ across known loads $\mathbf{Z}_L$.

E. Degrees of Freedom of an n_p Port Array

As the number of MOM basis functions N_B used to discretize the antennas grows large, one would expect that an equally large number of parameters would be needed to represent the current distribution $\mathbf{i}_A$ on the antennas. Here we illustrate that often a more concise representation is possible.

Consider the array in transmit mode where $\mathbf{e}^{\rm inc} = 0 \rightarrow \mathbf{v}_A^{\rm inc} = 0$. According to (7), $\mathbf{i}_A$ is a weighted sum of at most N_P linearly independent vectors spanned by the columns of $\boldsymbol{\xi} = \mathbf{Q}_{AA}^{-1}\mathbf{Q}_{AP}$, regardless of what is attached to the ports (loads or sources). Therefore, only N_P independent basis functions are needed to completely represent currents on the array. Next consider the receive mode with a fixed $\mathbf{e}^{\rm inc} \neq 0$. The incident field simply adds one additional basis vector in (7), meaning that $\mathbf{i}_S$ can be decomposed into a weighted sum of $N_P + 1$ fixed basis vectors, regardless of port termination.

For the receive mode when $\mathbf{e}^{\text{inc}}$ is not fixed, the number of required basis vectors is at most $N_P + N_E$, where N_E is the number of linearly independent $\mathbf{v}_A^{\text{inc}}$ that can exist, which may be large in practice. However, in some special cases, the $\mathbf{v}_A^{\text{inc}}$ are linearly dependent. For example, if the array consists of minimally scattering thin-wire dipoles [16] and $\mathbf{e}^{\text{inc}}(\hat{r})$ is a plane wave coming from direction $\hat{r}$ and oriented parallel to the dipoles, $\mathbf{v}_A^{\text{inc}}$ for each antenna is a scan angle dependent scalar times a constant vector. According to (7), the current $\mathbf{i}_A$ on each antenna requires at most one basis vector in addition to the N_P transmit mode vectors, meaning up to $2N_P$ vectors are needed to represent all current distributions on the array. In [10] it is correctly observed that one basis function per antenna is insufficient to represent antenna currents on a dipole array with parallel plane-wave excitation. However, our analysis shows that only *two* basis functions are needed per antenna, as long as they span the correct subspace.

F. Alternative Model Parameterizations

Although equivalent, there are times when other network parameterizations are desirable. Multiplying both sides of (8) by $\mathbf{Z}^{-1}$ results in the admittance formulation

$$\mathbf{i}_P = \underbrace{\mathbf{Z}^{-1}\mathbf{v}_P^{\text{oc}}}_{\mathbf{i}_P^{\text{sc}}} + \underbrace{\mathbf{Z}^{-1}}_{\mathbf{Y}}\mathbf{v}_P \tag{17}$$

where $\mathbf{Y}$ is the admittance matrix and $\mathbf{i}_P^{\text{sc}}$ is the current flowing into the ports due to the incident field when all ports are short-circuited. Substituting $\mathbf{i}_P$ from (17) into expression (9) for radiated fields,

$$\mathbf{e}(\mathbf{r}) = \mathbf{e}^{\text{inc}}(\mathbf{r}) + \underbrace{[\mathbf{e}^{\text{oc,scat}}(\mathbf{r}) + \mathbf{E}^{\text{oc}}(\mathbf{r})\mathbf{i}_P^{\text{sc}}]}_{\mathbf{e}^{\text{sc,scat}}} + \underbrace{\mathbf{E}^{\text{oc}}(\mathbf{r})\mathbf{Y}}_{\mathbf{E}^{\text{sc}}(\mathbf{r})}\mathbf{v}_P \tag{18}$$

where $\mathbf{E}^{\text{sc}}(\mathbf{r})$ are the transmit-mode short-circuit embedded patterns where the nth pattern (column) is obtained by placing a unit voltage source across the nth port and zero volts (short circuit) across the other ports.

The scattering parameter (S-parameter) formulation relates the ingoing waves $\mathbf{a}$ and outgoing waves $\mathbf{b}$ on the network ports, which are related to the port voltages and currents according to

$$\mathbf{v}_P = Z_0^{1/2}(\mathbf{a}_P + \mathbf{b}_P),\ \mathbf{i}_P = Z_0^{-1/2}(\mathbf{a}_P - \mathbf{b}_P) \tag{19}$$

where Z_0 is an arbitrary normalizing impedance. Substituting $\mathbf{v}_P$ and $\mathbf{i}_P$ from (19) into (8) and rearranging yields

$$\mathbf{b}_P = \underbrace{\sqrt{Z_0}(\mathbf{Z} + Z_0\mathbf{I})^{-1}\mathbf{v}_P^{\text{oc}}}_{\mathbf{b}_P^{\text{mc}}} + \underbrace{(\mathbf{Z} + Z_0\mathbf{I})^{-1}(\mathbf{Z} - Z_0\mathbf{I})}_{\mathbf{S}}\mathbf{a}_P \tag{20}$$

where $\mathbf{b}_P^{\text{mc}}$ is the outward traveling wave due to the incident field for matched circuits (loads with impedance Z_0) connected to all ports and $\mathbf{S}$ is the transmit S-parameter matrix of array. Substituting (20) into (19),

$$\mathbf{i}_P = Z_0^{-1/2}[(\mathbf{I} - \mathbf{S})\mathbf{a}_P - \mathbf{b}_P^{\text{mc}}] \tag{21}$$

which substituted into (9) yields

$$\mathbf{e}(\mathbf{r}) = \mathbf{e}^{\text{inc}}(\mathbf{r}) + \underbrace{\mathbf{e}^{\text{oc,scat}} - \frac{\mathbf{E}^{\text{oc}}(\mathbf{r})}{\sqrt{Z_0}}\mathbf{b}_P^{\text{mc}}}_{\mathbf{e}^{\text{mc,scat}}(\mathbf{r})} + \underbrace{\frac{\mathbf{E}^{\text{oc}}(\mathbf{r})}{\sqrt{Z_0}}(\mathbf{I} - \mathbf{S})}_{\mathbf{E}^{\text{mc}}(\mathbf{r})}\mathbf{a}_P \tag{22}$$

where $\mathbf{e}^{\text{mc,scat}}(\mathbf{r})$ is the scattered field due to incident field with matched loads on all ports and $\mathbf{E}^{\text{mc}}(\mathbf{r})$ are the matched circuit patterns.

G. Network Analysis of Reconfigurable Antennas

Network analysis is an attractive solution for analyzing reconfigurable antennas with a large number of possible states, since the number of required full-wave simulations can be kept to a minimum. In this section, we illustrate that if N_R out of $N_R + N_P$ ports are terminated with loads (such as reconfigurable elements), this simply creates a new effective array with N_P ports having modified network parameters and new radiation/reception patterns. Also, we use this framework to show that the impedance matrix of a non-reciprocal system is the same for transmit and receive mode and only the transmit and reception patterns are different.

Consider a reconfigurable antenna array with $N_R + N_P$ total ports, where N_R ports are terminated with loads (such as reconfigurable elements) and N_P are left accessible to be connected to transmit or receive RF chains. Letting vector ports 1 and 2 correspond to the accessible and reconfigurable terminations, respectively, we have

$$\begin{bmatrix}\mathbf{v}_1\\ \mathbf{v}_2\end{bmatrix} = \begin{bmatrix}\mathbf{Z}_{11} & \mathbf{Z}_{12}\\ \mathbf{Z}_{21} & \mathbf{Z}_{22}\end{bmatrix}\begin{bmatrix}\mathbf{v}_1^{\text{oc}}\\ \mathbf{v}_2^{\text{oc}}\end{bmatrix}. \tag{23}$$

Terminating port 2 with a network having the impedance matrix $\mathbf{Z}_L$, we have $\mathbf{v}_2 = -\mathbf{Z}_L\mathbf{i}_2$ and solving for $\mathbf{v}_1$

$$\mathbf{v}_1 = \underbrace{[\mathbf{Z}_{11} - \mathbf{Z}_{12}(\mathbf{Z}_{22} + \mathbf{Z}_L)^{-1}\mathbf{Z}_{21}]}_{\mathbf{Z}'}\mathbf{i}_1 + \underbrace{\mathbf{v}_1^{\text{oc}} - \mathbf{Z}_{12}(\mathbf{Z}_{22} + \mathbf{Z}_L)^{-1}\mathbf{v}_2^{\text{oc}}}_{\mathbf{v}^{\text{oc}\prime}} \tag{24}$$

which means that the loaded antenna system forms a new circuit with impedance matrix $\mathbf{Z}'$ and open-circuit voltage $\mathbf{v}^{\text{oc}\prime}$. The far-field of the array can be computed using (10) where

$$\mathbf{E}^{\text{oc}}(\hat{r})\mathbf{i}_P = \mathbf{E}_1^{\text{oc}}(\hat{r})\mathbf{i}_1 + \mathbf{E}_2^{\text{oc}}(\hat{r})\mathbf{i}_2 \tag{25}$$

and $\mathbf{E}_1^{\text{oc}}(\hat{r})$ and $\mathbf{E}_2^{\text{oc}}(\hat{r})$ are radiation pattern matrices for the accessible and loaded ports, respectively. Eliminating $\mathbf{i}_2$

$$\mathbf{e}(\mathbf{r}) = \mathbf{e}^{\text{inc}}(\mathbf{r}) + \{\underbrace{[\mathbf{E}_1^{\text{oc}}(\hat{r}) - \mathbf{E}_2^{\text{oc}}(\hat{r})(\mathbf{Z}_{22} + \mathbf{Z}_L)^{-1}\mathbf{Z}_{21}]}_{\mathbf{E}^{\text{oc}\prime}(\hat{r},\mathbf{Z}_L)}\mathbf{i}_1 + \underbrace{\mathbf{e}^{\text{oc,scat}}(\hat{r}) - \mathbf{E}_2^{\text{oc}}(\hat{r})(\mathbf{Z}_{22} + \mathbf{Z}_L)^{-1}\mathbf{v}_2^{\text{oc}}}_{\mathbf{e}^{\text{oc,scat}\prime}(\hat{r})}\} \times \exp\frac{(-jkr)}{r,} \tag{26}$$

indicating that the loaded array can be treated as a usual array as before except with modified open-circuit radiation patterns.

It is instructive to consider the case where the unloaded array and channel are reciprocal ($\mathbf{Z} = \mathbf{Z}^T$), but the loading is not ($\mathbf{Z}_L \neq \mathbf{Z}_L^T$). The unloaded open-circuit voltage can still be computed from (13), or

$$\begin{bmatrix} \mathbf{v}_1^{\rm oc} \\ \mathbf{v}_2^{\rm oc} \end{bmatrix} = \alpha \begin{bmatrix} \mathbf{E}_1^{\rm oc}(\hat{r})^T \mathbf{e}_0 \\ \mathbf{E}_2^{\rm oc}(\hat{r})^T \mathbf{e}_0 \end{bmatrix}. \tag{27}$$

Substituting into (24),

$$\mathbf{v}_2^{\rm oc\prime} = \alpha \mathbf{E}_1^{\rm oc}(\hat{r})^T \mathbf{e}_0 - \alpha \mathbf{Z}_{12}(\mathbf{Z}_{22}+\mathbf{Z}_L)^{-1} \mathbf{E}_2^{\rm oc}(\hat{r})^T \mathbf{e}_0, \tag{28}$$

$$= \alpha \underbrace{\left[\mathbf{E}_1^{\rm oc}(\hat{r}) - \mathbf{E}_2^{\rm oc}(\hat{r})(\mathbf{Z}_{22}+\mathbf{Z}_L^T)^{-1}\mathbf{Z}_{21}\right]^T}_{\mathbf{E}^{\rm oc\prime}(\hat{r},\mathbf{Z}_L^T)} \mathbf{e}_0. \tag{29}$$

Thus, although the radiation pattern $\mathbf{E}^{\rm oc\prime}(\hat{r}, \mathbf{Z}_L)$ in (26) is different from the reception pattern $\mathbf{E}^{\rm oc\prime}(\hat{r}, \mathbf{Z}_L^T)$, the same impedance matrix $\mathbf{Z}'$ in (24) is used for both transmit and receive modes.

H. Potential Sources of Inaccuracy

Although (8) and other network representations are exact, it is instructive to consider how improper application may lead to potential inaccuracy.

1) Isolated vs. Embedded Element Patterns: A common simplifying assumption in equivalent circuit models of antenna arrays is the use of *isolated* transmit and receive patterns, rather than precise embedded patterns. For an array composed of identical elements, this approach only requires a single pattern to be found followed by pattern multiplication with the array factor.

The operation of isolated elements is defined from (5) and (6) by replacing $\mathbf{Q}$ with the block matrix $\mathbf{Q}^{\rm iso}$, where

$$q_{mm'}^{\rm iso} = \begin{cases} q_{mm'}, & a(m) = a(m') \\ 0, & \text{otherwise} \end{cases} \tag{30}$$

and the function $n = a(m)$ maps the basis function index m to its associated antenna port n. Assuming isolated antennas in the transmit mode, $\mathbf{i}_A = -\mathbf{Q}_{AA}^{\rm iso\,-1}\mathbf{Q}_{AP}^{\rm iso}\mathbf{i}_P$ implies that the current $\mathbf{i}_A$ on an entire open-circuit antenna is zero. In the receive mode, a similar substitution of $\mathbf{Q} = \mathbf{Q}^{\rm iso}$ is made for $\mathbf{v}^{\rm oc}$ in (8), which leads to the observation that when $v_n^{\rm oc}$ is computed, only the currents induced by $v_{A,m}$ for $a(m) = n$ are used and currents on other antennas are treated as zero.

Antennas that exhibit negligible current when open-circuited, or $\mathbf{Q} \approx \mathbf{Q}^{\rm iso}$, are referred to as *minimally scattering* antennas [16], where the principle example is thin wire dipoles. Clearly for general antennas, $\mathbf{Q}$ will not be close to $\mathbf{Q}^{\rm iso}$, meaning that significant currents can flow on the surface of an open-circuited antenna. Since these currents will affect $\mathbf{e}^{\rm oc}$ and $\mathbf{v}^{\rm oc}$, assuming isolated patterns can lead to significant error in network computations.

2) Current Distribution on Loads and Sources: The network model in Fig. 2 allows arbitrary loads and sources to be connected to the ports. However, note that the model is only exact when the current densities on the ports have the same distribution as the basis functions that were chosen for computing $\mathbf{Q}$. When the current distributions on the ports are significantly altered, the matrices $\mathbf{Q}_{PP}$, $\mathbf{Q}_{PA}$ and $\mathbf{Q}_{AP}$ are also different, leading to error.

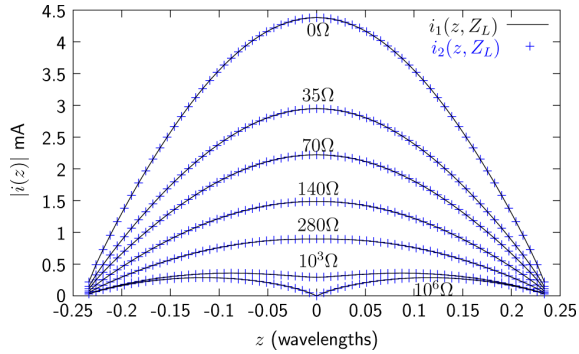

Fig. 4. Current distribution on a single dipole antenna for different loading, where i_1 is the predicted value using the transmit-mode current distribution and i_2 is from direct receive-mode simulation.

III. Numerical Examples

This section provides numerical examples, not only to validate the previous analytical results, but also to help provide intuition on the behavior of the multi-antenna systems with coupling.

A. Single Antenna: Transmission vs. Reception

First, we study a simple single-antenna MOM simulation. Although somewhat trivial, this case demonstrates the important principle that the difference in transmit and receive current distributions on an antenna is exactly predicted by the open-circuit current distribution.

The Numerical Electromagnetics Code Version 2 (NEC2) [17] was used for simulations of a single z-directed dipole with length $\ell = 0.475\lambda$ and radius $a = 0.001\lambda$. The antenna was first simulated in the transmit mode with a 1 V source placed across the terminals and the resulting current on the antenna $i^{\rm TX}(z)$ and z-directed far-zone E fields versus azimuth angle ϕ were stored. Second, the antenna was simulated in receive mode with a plane wave coming from azimuth angle ϕ with $\mathbf{e}_0 = 1\hat{z}\ \mathrm{V}/\lambda$ for loads $Z_L \in \{0, 35, 70, 140, 280, 10^3, 10^6\}\ \Omega$ giving antenna current $i^{\rm RX}(z, Z_L)$.

Fig. 4 plots the current distribution on the antenna for different loads obtained in two ways. First, the load current in the receive mode combined with the open-circuit current ($Z_L = 10^6\ \Omega$) is used to compute the current everywhere on the antenna, or $i_1(z, Z_L) = i^{\rm TX}(z)/i^{\rm TX}(0) i^{\rm RX}(0, Z_L) + i^{\rm RX}(z, 10^6\ \Omega)$, where $z = 0$ is the load position. In this first case, the current can be computed for any receive load using just two basis functions. Second, the current is taken directly from receive mode simulations $i_2(z, Z_L) = i^{\rm RX}(z, Z_L)$.

The result indicates nearly perfect agreement in the current distribution for the receive mode simulation for different loads and the value predicted from transmit-mode quantities. This also confirms that for the chosen incident field, the current distribution on the antenna is the sum of only two independent basis functions.

B. Two Dipole Simulation

Next, we consider the case of two dipoles and show that load voltages in the receive mode are exactly predicted by

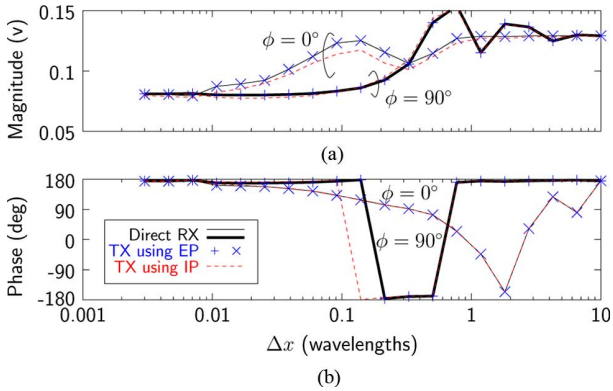

Fig. 5. Voltage on antenna 1 for simulations of coupled 2-dipole simulations, computed using direct receive (RX) mode simulations, using transmit (TX) simulations with embedded patterns (EP) and TX simulations using isolated patterns (IP).

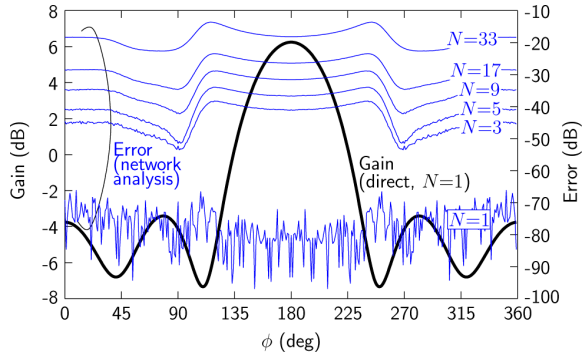

Fig. 6. Directional gain of a 7-element parasitic dipole array (thick line) and fractional deviation of gain when network analysis is used (thin lines), where N is the number of fixed-length segments used for the load.

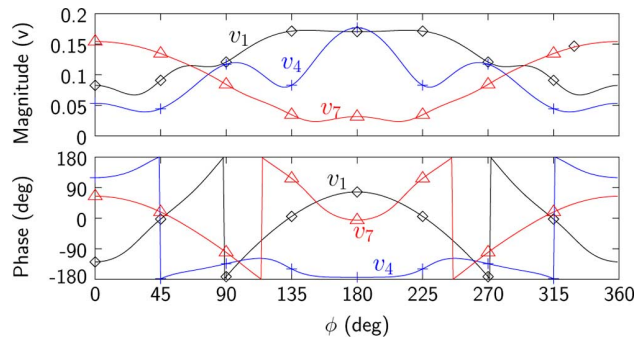

Fig. 7. Load voltages for the terminated 7-element array for plane wave excitation arriving from azimuth angle ϕ. Solid lines show voltages computed using transmit-mode quantities with network analysis and points show values from direct receive-mode simulations.

transmit-mode only quantities, regardless of dipole separation. NEC2 simulations were performed for two z-directed dipoles separated by distance Δx with $\ell = 0.475\lambda$ and $a = 0.001\lambda$. First, the array is analyzed in the transmit mode, where the quantities $\mathbf{Y}$ and $\mathbf{E}^{\rm oc}(\hat{r})$ are found by performing N_P simulations, where for the kth simulation, port k is driven with a 1 V source across the terminals and short circuits (PEC) are placed across the terminals of the other elements. The resulting vector of terminal currents is denoted $\mathbf{i}^{(k)}$, giving the kth column of the admittance matrix $\mathbf{Y}$. Far-fields are $\mathbf{e}^{\rm sc}(\mathbf{r}) = \mathbf{e}^{\rm sc}(\hat{r})\exp(-jkr)/r$ and the far-field pattern $\mathbf{e}^{\rm sc}(\hat{r})$ is stored for the azimuthal plane $(\hat{r}(\phi) = \hat{x}\cos\phi + \hat{y}\sin\phi)$, yielding the kth column of $\mathbf{E}^{\rm sc}(\phi)$. After performing a simulation for each port, the impedance matrix is computed with $\mathbf{Z} = \mathbf{Y}^{-1}$ and $\mathbf{E}^{\rm oc}$ is found from (18) as $\mathbf{E}^{\rm oc}(\phi) = \mathbf{E}^{\rm sc}(\phi)\mathbf{Z}$. Second, the array is analyzed directly in the receive mode by terminating each antenna with $Z_L = 50\ \Omega$ and running a separate simulation for a plane wave arriving in the xy plane from azimuthal angle ϕ with $\mathbf{e}_0 = 1\hat{z}\ \mathrm{V}/\lambda$.

The load voltage on one of the antennas in the receive mode versus the arrival angle ϕ is obtained three different ways. In the first case, the open-circuit voltage of the array for arrival angle ϕ is computed using the embedded transmit patterns $\mathbf{E}^{\rm oc}(\hat{r})$ according to (13), after which the loaded voltage for arbitrary load impedance $\mathbf{Z}_L$ can be computed. In the second case, we apply the same procedure, except that the open-circuit voltage is computed using the transmit patterns of *isolated* elements (i.e., one antenna is driven with 1 V and the other is removed). In the third case, the voltages from direct receive-mode simulations are used.

Fig. 5(a) and (b) show the amplitude and phase, respectively, of the voltage on antenna 1 for $\phi = 0$ and $\phi = 90°$. The result shows exact agreement between the transmit and receive mode cases when the embedded patterns are used to obtain $\mathbf{v}^{\rm oc}$. Also, since the results are not normalized, the agreement validates the scaling constant in (13) relating $\mathbf{v}^{\rm oc}$ to the embedded open-circuit transmit patterns. When isolated patterns are used, however, a small amount of error (mainly in the amplitude) is created for dipoles separated by less than 0.3λ, which may or may not be tolerable depending on the application.

C. Simulation of a Parasitic Array

In this section we demonstrate the behavior of a larger array with parasitic loading. We also study the effect of a varying port current distribution that can affect the accuracy of the network analysis computations.

Moment method simulations of a 7-element uniform linear array of dipoles were performed using NEC2 identical to the antennas in Sections III-A and III-B, except a fixed inter-element spacing of $\Delta x = 0.1\lambda$ was used. We also consider the case of a distributed load occupying $N_{\rm S,load}$ of the segments at the middle of the antenna, allowing the port current distribution to be changed.

First, we demonstrate how the size of the load can affect the accuracy of network computations. Fig. 6 depicts the directive gain of the array for $N_{\rm S,load} = 1$ (thick black line) obtained from a single transmit-mode NEC2 simulation when the center element (antenna 4) is driven with an active source, antennas 1–3 are terminated with $Z_L = 73\ \Omega$ and antennas 5-7 are terminated with $Z_L = j30\ \Omega$. Next, directional gain was computed with network analysis using $\mathbf{Z}$ and $\mathbf{E}^{\rm oc}(\phi)$ and the results of Section II-G. The fractional error of the network analysis solution compared to the direct solution is shown as thin lines in the plot. For small $N_{\rm S,load}$, network analysis and the direct solution give nearly identical results, whereas for increasing $N_{\rm S,load}$ moderate error is obtained.

Finally, we illustrate again that transmit-mode quantities can precisely predict the receive-mode response. Fig. 7 plots

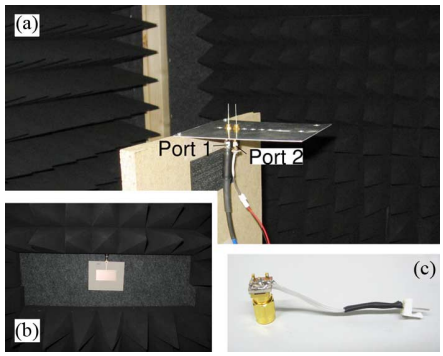

Fig. 8. Photos of the parasitic reconfigurable antenna measured in a compact anechoic chamber: (a) parasitic array where ports 1 and 2 are connected to the receiver and a varactor diode load (b) reference patch antenna used to illuminate the array (c) reconfigurable varactor diode circuit.

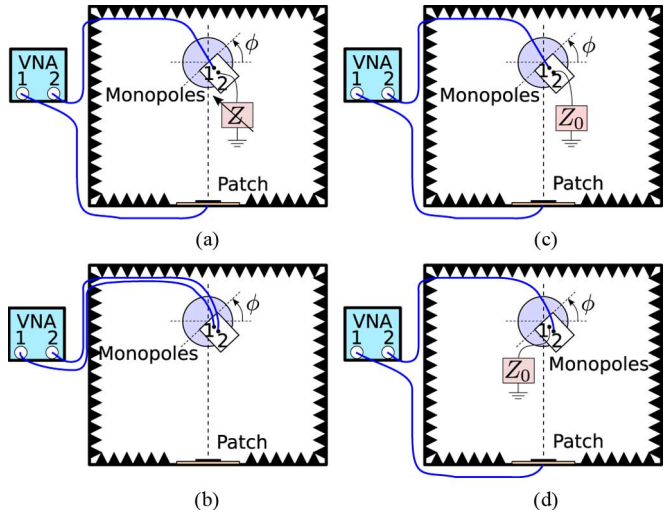

Fig. 9. Measurement cases taken in an anechoic chamber to illustrate antenna computations.

the terminal voltage on three of the antennas for a single plane wave, where antennas 1–4 and 5–7 are terminated with $Z_L = 73\ \Omega$ and $j30\ \Omega$, respectively and $N_{\mathrm{S,load}} = 1$. The receive load voltage was computed with network analysis using transmit mode quantities (solid lines) and with direct receive-mode NEC2 simulations for plane waves at specific angles (points). Nearly exact agreement is obtained, indicating that the receive-mode behavior can be computed from the usual transmit-mode quantities.

IV. Experimental Example

This section provides a simple experiment that confirms that transmit-mode quantities can be used to predict receive mode behavior in real antenna systems. The chosen antenna is a reconfigurable parasitic antenna that has application in adaptive matching and pattern synthesis.

Fig. 8(a) depicts the antenna system to be analyzed, consisting of one monopole antenna connected to a receiver (Port 1) and a coupled parasitic monopole terminated with a varactor diode having variable 0–5 V reverse bias (Port 2), where the varactor diode circuit is depicted in Fig. 8(c). The monopoles are spaced by 1 cm which is approximately 0.07λ at the operating frequency of 2.2 GHz. Antenna measurements were performed at 2.2 GHz in the $2\ \mathrm{m} \times 2\ \mathrm{m} \times 2\ \mathrm{m}$ anechoic chamber depicted where a low transmit power of 0 dBm was used to ensure linearity of the varactor diode. The reference antenna for the experiment was a patch antenna mounted on a chamber wall, depicted in Fig. 8(b).

Measurements were performed with a two-port Rohde&Schwarz VNB20 vector network analyzer outside of the chamber, connected to the antennas with phase-stable cables. To avoid having to reroute cables between the various measurements, three cables were run from the VNA location to the antenna ports inside the chamber, where two 3 m cables were run to the monopole antenna ports and one 6 m cable to the patch antenna. Note that the VNA was calibrated for each configuration to obtain S-parameters with respect to the ends of the cables.

First, the receive antenna was characterized directly in the pure receive mode using the arrangement in Fig. 9(a), where for each rotation angle $\phi \in \{-90°, -80°, \ldots, 90°\}$, biases of $V_{\mathrm{bias}} \in \{0, 0.1, 0.2, \ldots, 5\}\ V$ were successively placed on the diode and $S_{21}^{(a)}(\phi, V_{\mathrm{bias}}) = b_{P1}/a$ was measured, where a is the complex amplitude of the constant incident wave fed to the patch and the superscript "(a)" denotes configuration (a) in Fig. 9.

Next, we show that the antenna system can be characterized using pure transmit-mode quantities. Consider the reconfigurable antenna to be a two-port element, where Port 2 is terminated with the varactor diode load having the bias-dependent reflection coefficient $\Gamma_L(V_{\mathrm{bias}})$. Using (20) and noting that $a_{P2} = \Gamma_L(V_{\mathrm{bias}}) b_{P2}$, the outgoing wave from Port 1 of the antenna is

$$b_{P1} = \frac{S_{12}\Gamma_L}{1 - S_{22}\Gamma_L} b_{P2}^{\mathrm{mc}} + b_{P1}^{\mathrm{mc}}. \tag{31}$$

Reflection of the varactor circuit with respect to V_{bias} is performed with a 1-port VNA measurement to obtain $\Gamma_L(V_{\mathrm{bias}})$. S-parameters $\mathbf{S}$ of the 2-port monopole array are found using the usual transmit-mode configuration in Fig. 9(b), giving the values $S_{11} = -0.45 + j0.49$, $S_{12} = S_{21} = 0.050 - j0.32$ and $S_{22} = -0.45 + j0.48$ as required in (31).

Next, the source waves b_{P1}^{mc} and b_{P2}^{mc} must be determined in the presence of the transmitting patch antenna for each illumination angle ϕ. The quantity b_{P1}^{mc} is found using the reciprocal arrangement in Fig. 9(c), where for each angle Monopole 1 is excited with an incident wave having complex amplitude a, Monopole 2 is terminated with Z_0 and the wave received by the patch is measured. This measurement gives

$$S_{12}^{(c)}(\phi) = S_{21}^{(c)}(\phi) = \left.\frac{b_{P1}(\phi)}{a}\right|_{\substack{a_{P1}=0 \\ a_{P2}=0}} = \frac{b_{P1}^{\mathrm{mc}}(\phi)}{a} \tag{32}$$

indicating that b_{P1}^{mc} can be obtained by just scaling the transmit-mode quantity $S_{12}^{(c)}$. Similarly, the arrangement in Fig. 9(d) is used to obtain $b_{P2}^{\mathrm{mc}}/a = S_{12}^{(d)}$. Substituting into (31),

$$S_{21}^{(a)}(\phi, V_{\mathrm{bias}}) = \frac{S_{12}\Gamma_L(V_{\mathrm{bias}})}{1 - S_{22}\Gamma_L(V_{\mathrm{bias}})} S_{12}^{(d)}(\phi) + S_{12}^{(c)}(\phi). \tag{33}$$

Fig. 10 compares direct receive-mode measurement of $S_{21}^{(a)}(\phi, V_{\mathrm{bias}})$ and the value computed with network analysis

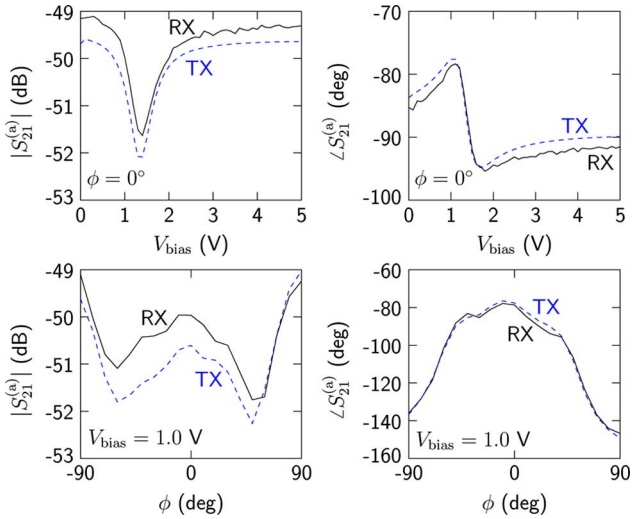

Fig. 10. Received signal on a parasitically controlled reconfigurable antenna obtained by direct measurement in the receive mode (RX) and predicted using network analysis and measured transmit-mode quantities (TX), where ϕ is the rotation angle of the antenna and V_{bias} is the reverse bias placed on the varactor diode element.

in (31) using transmit-mode quantities, where cases of both the bias and sweep angle being held constant are shown. Good agreement is obtained and the small discrepancies are to be expected due to separate measurements being performed, where disconnection and reconnection of a single cable caused as much as ± 0.2 dB and $\pm 2°$ variation in measured S-parameters.

V. Conclusion

This paper has analyzed antenna arrays consisting of general PEC surfaces based on a rigorous method of moments (MOM) formulation, showing that equivalent circuit models are exact from the standpoint of electromagnetic wave theory. The results also indicate that receive-mode operation of arrays is exactly predicted by employing the usual transmit-mode network parameters (Z, Y, or S-parameters) and an excitation-dependent source term. For the case of reciprocal antennas and far-field sources, this source term is completely determined by the transmit-mode embedded radiation patterns of the array. Two sources of possible error in equivalent network models were identified, namely using isolated instead of embedded element patterns and modeling the incorrect current mode at the ports. Numerical and experimental examples demonstrated the validity of the analytical results and the effect of the sources of error.

References

[1] C. Waldschmidt, S. Schulteis, and W. Wiesbeck, "Complete RF system model for analysis of compact MIMO arrays," *IEEE Trans. Veh. Technol*, vol. 53, pp. 579–586, May 2004.

[2] J. W. Wallace and M. A. Jensen, "Mutual coupling in MIMO wireless systems: A rigorous network theory analysis," *IEEE Trans. Wireless Commun*, vol. 3, pp. 1317–1325, Jul. 2004.

[3] M. L. Morris and M. A. Jensen, "Network model for MIMO systems with coupled antennas and noisy amplifiers," *IEEE Trans. Antennas Propag*, vol. 53, pp. 545–552, Feb. 2005.

[4] B. K. Lau, J. B. Andersen, G. Kristensson, and A. F. Molisch, "Impact of matching network on bandwidth of compact antenna arrays," *IEEE Trans. Antennas Propag*, vol. 54, pp. 3225–3238, Nov. 2006.

[5] V. Papamichael and C. Soras, "MIMO antenna modelling using the effective length matrices," *Progr. Electromagn. Res. C*, vol. 10, pp. 111–127, Oct. 2009.

[6] A. T. D. Hoop, "The N -port receiving antenna and its equivalent electrical network," *Philips Res. Rep.*, vol. 30, pp. 302–315, 1975.

[7] I. Gupta and A. Ksienski, "Effect of mutual coupling on the performance of adaptive arrays," *IEEE Trans. Antennas Propag*, vol. 31, pp. 785–791, Sep. 1983.

[8] J. Van Bladel, "On the equivalent circuit of a receiving antenna," *IEEE Antennas Propag. Mag.*, vol. 44, pp. 164–165, Feb. 2002.

[9] P.-S. Kildal, "Equivalent circuits of receive antennas in signal processing arrays," *Microwave Opt. Technol. Lett.*, vol. 21, pp. 244–246, May 1999.

[10] R. S. Adve and T. K. Sarkar, "Compensation for the effects of mutual coupling on direct data domain adaptive algorithms," *IEEE Trans. Antennas Propag*, vol. 48, pp. 86–94, Jan. 2000.

[11] A. W. Love, "Comment on the equivalent circuit of a receiving antenna," *IEEE Trans. Antennas Propag*, vol. 44, pp. 124–125, Oct. 2002.

[12] W. Geyi, "Derivation of equivalent circuits for receiving antenna," *IEEE Trans. Antennas Propag*, vol. 52, pp. 1620–1623, Jun. 2004.

[13] H. T. Hui, "A new definition of mutual impedance for application in dipole receiving antenna arrays," *IEEE Antennas Wireless Propag. Lett*, vol. 3, pp. 364–367, Mar. 2004.

[14] H.-S. Lui, H. T. Hui, and M. S. Leong, "A note on the mutual-coupling problems in transmitting and receiving antenna arrays," *IEEE Antennas Propag. Mag.*, vol. 51, pp. 171–176, Oct. 2009.

[15] J. A. Kong, *Electromagnetic Wave Theory*, 2nd ed. New York: Wiley, 1990.

[16] W. Wasylkiwskyj and W. Kahn, "Theory of mutual coupling among minimum-scattering antennas," *IEEE Trans. Antennas Propag*, vol. 18, pp. 204–216, Mar. 1970.

[17] [Online]. Available: http://www.nec2.org

Jon W. Wallace (S'99–M'03) received the B.S. (*summa cum laude*) and Ph.D. degrees in electrical engineering from Brigham Young University (BYU), Provo, UT, in 1997 and 2002, respectively.

He received the National Science Foundation Graduate Fellowship in 1998 and worked as a Graduate Research Assistant at BYU until 2002. From 2002 to 2003, he was with the Mobile Communications Group, Vienna University of Technology, Vienna, Austria. From 2003 to 2006, he was a Research Associate with the BYU Wireless Communications Laboratory. Since 2006, he has been an Assistant Professor of electrical engineering at Jacobs University, Bremen, Germany. His current research interests include MIMO wireless systems, physical-layer security, cognitive radio and UWB systems.

Dr. Wallace is serving as an Associate Editor of the IEEE Transactions on Antennas and Propagation and is a Co-Guest Editor of the Special Issue on Multiple-Input Multiple-Output (MIMO) Technology.

Rashid Mehmood (S'05) received the B.Sc. degree (*cum laude*) in communication systems engineering from the Institute of Space Technology (IST), Pakistan, in 2007 and the M.Sc. degree in electrical engineering from Jacobs University Bremen (JUB), Bremen, Germany, in 2010.

From 2007 to 2008, he worked as a Research Associate at IST and supervised various undergraduate laboratories. From 2008 to 2010, he worked as a Research Assistant in several laboratories at JUB and external companies. His current research interests include reconfigurable aperture antennas, antenna optimization and wireless and optical communications.

Mr. Mehmood was a recipient of the 2009 IEEE AP-S Undergraduate Research Award.